JOC*Article*

Molecular-Recognition Properties of a Water-Soluble Cucurbit[6]uril Analogue

Jason Lagona,[†] Brian D. Wagner,*[,‡] and Lyle Isaacs*[,†]

Department of Chemistry and Biochemistry, University of Maryland, College Park, Maryland 20742, and Department of Chemistry, University of Prince Edward Island, Charlottetown, Prince Edward Island, Canada C1A 4P3

lisaacs@umd.edu; bwagner@upei.ca

Received November 4, 2005

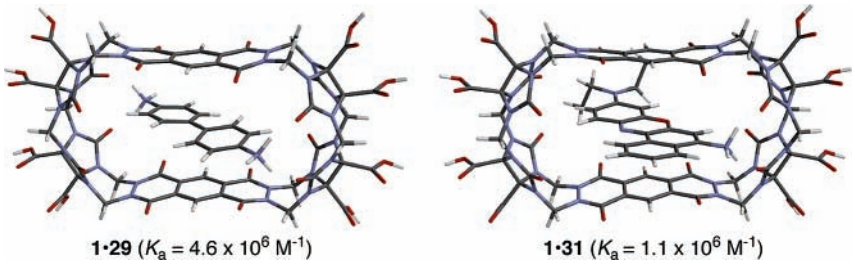

The molecular-recognition properties of the cucurbit[6]uril analogue (**1**) in aqueous buffer (sodium acetate, 50 mM, pH 4.74, 25 °C) toward a variety of guests including alkanediamines (**6**−**12**), aromatics (**14**−**32**), amino acids (**33**−**36**), and nucleobases (**37**−**42**) were studied by fluorescence spectroscopy. For the alkanediamines studied ($H_2N(CH)_nNH_2$, n = 6, 7, 8, 9, 10, 11, 12), the association constants increase as the length of the alkane (n) is increased. Host **1** is capable of forming strong complexes with guests containing aromatic rings with association constants (K_a) ranging from 10^2 to 10^6 M^{-1} as a result of the favorable $\pi-\pi$ interactions that occur between host **1** and the aromatic rings of the guest when bound in the cavity of **1**. Biologically relevant guests such as amino acids and nucleobases are also bound in the cavity of **1** with K_a values ranging from 10^3 to 10^6 M^{-1}. Consequently, cucurbit[6]uril analogue **1** functions as a versatile fluorescent sensor for the presence of a wide range of chemically and biologically important substances in aqueous solution including nitroaromatics, neurotransmitters, amino acids, and nucleobases.

Introduction

Cucurbit[6]uril (CB[6]) is a macrocyclic compound comprising 12 methylene bridges connecting six glycoluril units (Figure 1a,b). Since the elucidation of the structure of CB[6] by Mock in 1981, its outstanding molecular-recognition properties have been described in a series of reports, most notably from the groups of Mock,[1−3] Buschmann,[4,5] and Kim.[6−8] The relative rigidity of the CB[6] framework results in highly selective recognition properties toward cationic and hydrophobic species (e.g., alkanediamines) through noncovalent interactions including ion−dipole, hydrogen-bonding, and the hydrophobic effect. The detection of CB[6]·guest complexes was first reported for alkylammonium ions on the basis of experimental evidence from ^{1}H NMR,[2] UV/vis,[9] and calorimetry.[10] Since then, the binding of CB[6] to a wide variety of species, including alkali metal cations,[4] amino acids and amino alcohols,[11] and amino azabenzenes,[12] has been reported.

Unfortunately, underivatized CB[6] is not fluorescent and, therefore, cannot be monitored directly by fluorescence spectroscopy. Consequently, the fluorescence experiments performed

[†] University of Maryland.
[‡] University of Prince Edward Island.

(1) Freeman, W. A.; Mock, W. L.; Shih, N. Y. *J. Am. Chem. Soc.* **1981**, *103*, 7367−7368.
(2) Mock, W. L.; Shih, N. Y. *J. Org. Chem.* **1986**, *51*, 4440−4446.
(3) Mock, W. L. *Top. Curr. Chem.* **1995**, *175*, 1−24.
(4) Buschmann, H. J.; Cleve, E.; Schollmeyer, E. *Inorg. Chim. Acta* **1992**, *193*, 93−97.
(5) Hoffmann, R.; Knoche, W.; Fenn, C.; Buschmann, H.-J. *J. Chem. Soc., Faraday Trans.* **1994**, *90*, 1507−1511.
(6) Jon, S. Y.; Selvapalam, N.; Oh, D. H.; Kang, J.-K.; Kim, S.-Y.; Jeon, Y. J.; Lee, J. W.; Kim, K. *J. Am. Chem. Soc.* **2003**, *125*, 10186−10187.
(7) Kim, K. *Chem. Soc. Rev.* **2002**, *31*, 96−107.
(8) Lee, J. W.; Samal, S.; Selvapalam, N.; Kim, H.-J.; Kim, K. *Acc. Chem. Res.* **2003**, *36*, 621−630.
(9) Hoffmann, R.; Knoche, W.; Fenn, C.; Buschmann, H.-J. *J. Chem. Soc., Faraday Trans.* **1994**, *90*, 1507−1511.
(10) Meschke, C.; Buschmann, H. J.; Schollmeyer, E. *Thermochim. Acta* **1997**, *297*, 43−48.
(11) Buschmann, H. J.; Jansen, K.; Schollmeyer, E. *Thermochim. Acta* **1998**, *317*, 95−98.
(12) Neugebauer, R.; Knoche, W. *J. Chem. Soc., Perkin Trans. 2* **1998**, 529−534.

10.1021/jo052294i CCC: $33.50
Published on Web 01/06/2006

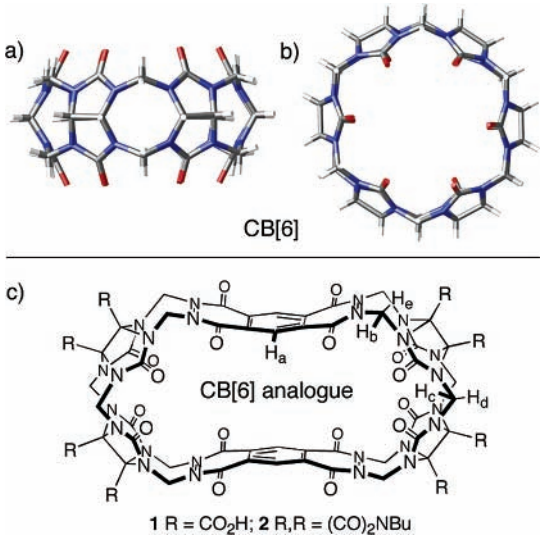

FIGURE 1. Representation of the X-ray crystal structure of CB[6]:[1] (a) side view and (b) top view. (c) Chemical structures of CB[6] analogues **1** and **2**. The labeled hydrogens on the CB[6] analogue **1** are used to denote those resonances in their ^{1}H NMR spectra (vide infra).

to date with CB[6] involved the use of fluorescent guests. Such experiments have been performed by the groups of Wagner,[13] Kim,[6,14] Buschmann,[15] Nau,[16] Kaifer,[17] and Urbach.[18] For example, Wagner and Buschmann independently reported fluorescence experiments using a mixture of 1-anilinonaphthalene-8-sulfonate and CB[6] in the solid state. A second approach toward the determination of the association constants of host−guest complexes using UV/vis or fluorescence spectroscopy involves the use of an indicator-displacement assay that consists of a pH- or solvatochromic-sensitive indicator.[19] This indicator (usually a fluorescent dye) forms a complex with the host but upon addition of a competitive guest is displaced, which changes its optical properties. This approach has not yet been applied in CB[*n*] chemistry. Our approach to CB[*n*] fluorescent sensors relies on the incorporation of a fluorophore into the CB skeleton, which would result in a universal detection scheme with a potentially wide dynamic range and high sensitivity.[20−22]

The synthesis of the fluorescent CB[*n*] analogues is carried out using a building block approach which allows for control over size, shape, and solubility of the resulting macrocycles.[20−23] The X-ray crystal structure of CB[6] analogue **1** illustrates the elongated shape of the CB[6] analogues (Figure 2), with dimensions of 5.90 × 11.15 × 6.92 Å; in contrast, CB[6] has a cylindrical-shaped cavity. We envisioned that the CB[*n*] analogues would possess unusual molecular-recognition properties including tight binding, high selectivity, and slow dynamics. Furthermore, we hoped that the CB[*n*] analogues would combine the desirable features of two important classes of host molecules, namely, CB[*n*] and cyclophanes.[24] As a result of the incorporation of aromatic walls, the CB[*n*] analogues are structurally similar to cyclophanes, but the carbonyl-lined portals resemble the CB[*n*] family. CB[*n*] analogues are preorganized to recognize guests molecules through a wide range of noncovalent interactions and are fluorescent. These host molecules, therefore, define a versatile platform to study the binding properties of a wide variety of chemically and biologically important guest molecules, including alkylamines, arylamines, dyes, amino acids, peptides, and nucleotides, using fluorescence spectroscopy. Furthermore, the potential to covalently attach these CB[*n*] analogues to a solid-phase support through their carboxylic acid derived functional groups would allow their use as fluorescent chip-based sensors in the detection of specific organic molecules such as explosives, neurotransmitters, proteins, and dyes.

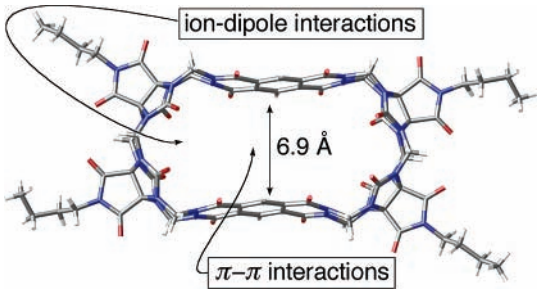

FIGURE 2. X-ray crystal structure of CB[6] analogue **2**.[20]

In this paper, we probe further into the molecular-recognition properties of the water-soluble CB[6] analogue (**1**) and its possible application as a fluorescent sensor for chemically and biologically important amines.[21,25] Herein, we report the binding constants of several different types of guests toward CB[6] analogue **1** in aqueous solution on the basis of the results from fluorescence titration experiments. We analyze these structure−activity data to elucidate the key factors (sterics, electrostatics, hydrophobicity, etc.) influencing the ability of **1** to complex with organic molecules.

Results and Discussion

Binding Properties of CB[6] Analogue 1 with 1,6-Hexanediamine (6). In this section we use 1,6-hexanediamine (**6**) as a model guest for **1** because it is the prototypical guest for the CB[*n*] family and to calibrate our analytical techniques (NMR, UV/vis, and fluorescence) before proceeding to study a wide variety of guests (vide infra).

(13) Wagner, B. D.; MacRae, A. I. *J. Phys. Chem. B* **1999**, *103*, 10114−10119. Wagner, B. D.; Fitzpatrick, S. J.; Gill, M. A.; MacRae, A. I.; Stojanovic, N. *Can. J. Chem.* **2001**, *79*, 1101−1104. Wagner, B. D.; Stojanovic, N.; Day, A. I.; Blanch, R. J. *J. Phys. Chem. B* **2003**, *107*, 10741−10746.

(14) Jun, S. I.; Lee, J. W.; Sakamoto, S.; Yamaguchi, K.; Kim, K. *Tetrahedron Lett.* **2000**, *41*, 471−475.

(15) Buschmann, H.-J.; Wolff, T. *J. Photochem. Photobiol., A* **1999**, *121*, 99−103.

(16) Marquez, C.; Huang, F.; Nau, W. M. *IEEE Trans. Nanobiosci.* **2004**, 39−45.

(17) Sindelar, V.; Cejas, M. A.; Raymo, F. M.; Kaifer, A. E. *New J. Chem.* **2005**, *29*, 280−282. Sindelar, V.; Cejas, M. A.; Raymo, F. M.; Chen, W.; Parker, S. E.; Kaifer, A. E. *Chem.−Eur. J.* **2005**, *11*, 7054−7059.

(18) Bush, M. E.; Bouley, N. D.; Urbach, A. R. *J. Am. Chem. Soc.* **2005**, *127*, 14511−14517.

(19) Houk, R. J. T.; Tobey, S. L.; Anslyn, E. V. *Top. Curr. Chem.* **2005**, *255*, 199−229. Wiskur, S. L.; Ait-Haddou, H.; Lavigne, J. J.; Anslyn, E. V. *Acc. Chem. Res.* **2001**, *34*, 963−972.

(20) Lagona, J.; Fettinger, J. C.; Isaacs, L. *Org. Lett.* **2003**, *5*, 3745−3747.

(21) Wagner, B. D.; Boland, P. G.; Lagona, J.; Isaacs, L. *J. Phys. Chem. B* **2005**, *109*, 7686−7691.

(22) Lagona, J.; Fettinger, J. C.; Isaacs, L. *J. Org. Chem.* **2005**, *70*, 10381−10392.

(23) Day, A. I.; Arnold, A. P.; Blanch, R. J. *Molecules* **2003**, *8*, 74−84. Zhao, Y.-J.; Xue, S.-F.; Zhang, Y.-Q.; Zhu, Q.-J.; Tao, Z.; Zhang, J.-X.; Wei, Z.-B.; Long, L.-S. *Huaxue Xuebao* **2005**, *63*, 913−918.

(24) Diederich, F. *Cyclophanes*; Royal Society of Chemistry: Cambridge, England, 1991. Stauffer, D. A.; Barrans, R. E., Jr.; Dougherty, D. A. *J. Org. Chem.* **1990**, *55*, 2762−2767.

(25) Feuster, E. K.; Glass, T. E. *J. Am. Chem. Soc.* **2003**, *125*, 16174−16175. Greene, N. T.; Morgan, S. L.; Shimizu, K. D. *Chem. Commun.* **2004**, 1172−1173. Zhang, C.; Suslick, K. S. *J. Am. Chem. Soc.* **2005**, *127*, 11548−11549.

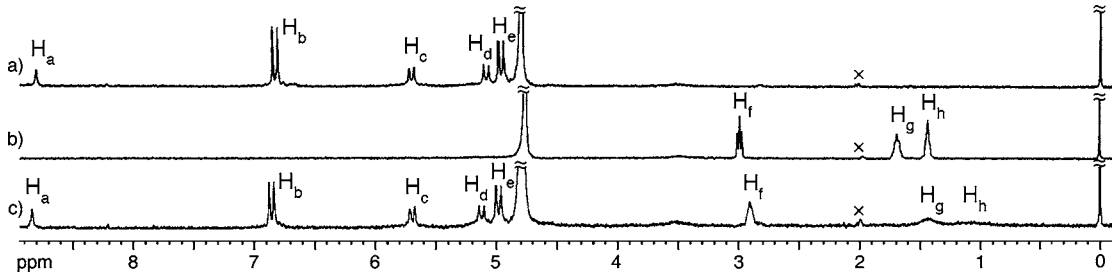

FIGURE 3. ^{1}H NMR spectra (400 MHz, 25 °C, 50 mM sodium acetate buffered D_2O, pD 4.74) for (a) **1** (1 mM), (b) **6** (1 mM), and (c) **1** (0.5 mM) and **6** (0.5 mM). × = OAc.

^{1}H NMR Study. The distance between the carbonyl portals of CB[6] is ≈6.0 Å; accordingly, alkanediamines with a commensurate N···N distance have the highest affinities toward CB[6]. For example, both 1,6-hexanediamine (**6**) and 1,5-pentanediamine (**5**) bind to CB[6] with high affinity ($K_a \approx 10^6$ M^{-1}) because the hydrophobic aliphatic portion of the guest resides completely in the cavity of the CB[6].[2] The ^{1}H NMR spectrum of a 1:1 mixture of diamine and CB[6] shows characteristic upfield shifts of the aliphatic portion of **6** on the order of ≈0.8 ppm when bound inside the cavity of CB[6].[2] Initially, we hypothesized that CB[6] analogue **1** would bind alkanediamines in a similar fashion with the $-(CH_2)_n-$ thread stretched between the two carbonyl portals. We hoped that the elongated shape of **1** might even allow the simultaneous binding of two alkanediamines in the hydrophobic cavity of **1** resulting in the formation of a ternary complex! The ^{1}H NMR spectra of **1**, **6**, and a 1:1 mixture of **1** and **6** are shown in Figure 3. The ^{1}H NMR spectrum of the mixture of **1** and **6** shows distinct upfield shifts (≈0.2 ppm) and broadening of the resonances corresponding to the protons on the β and γ carbons (H_g and H_h, respectively) of the aliphatic portion of guest **6**. Even though the protons on the α carbon (H_f) relative to the $-NH_3^+$ also show broadening, the upfield shift is not as dramatic because these methylene protons are the furthest away from the shielding region defined by the aromatic rings lining the cavity of host **1**. This broadening is due to the equilibrium process between free and bound 1,6-hexanediamine (**6**) being in the intermediate exchange regime on the chemical shift time scale. The resonances for the protons on **1** also show small shifts in the ^{1}H NMR spectrum upon complexation with diamine **6**. For example, the resonance corresponding to the aromatic protons (H_a) on the bis(phthalhydrazide) walls shifts downfield most likely because the binding of **6** in the cavity of **1** results in a geometrical change in the bis(phthalhydrazide) walls. A similar downfield shift is observed for the resonances for the diastereotopic protons (H_b) on the methylene bridges connecting the bis(phthalhydrazide) and the glycoluril. These protons are directed toward the interior of the cavity of host **1**. In addition to providing information on the structure of the **1·6** complex, these shifts as a function of concentration allowed us to determine the association constant of **1·6**.

We performed an NMR titration experiment in which the change in the shift of the resonance corresponding to the aromatic proton (H_a) was monitored as a function of the concentration of **6**. When these data are fit to a 1:1 binding model using a nonlinear least-squares analysis, we obtained $K_a = 630 \pm 40$ M^{-1} for **1·6**. Despite the fact that the titration data fit well to a 1:1 binding model, we wanted to obtain stronger evidence for the stoichiometry of the **1·6** complex. For this purpose, we performed a Job-plot analysis at a fixed total concentration of 1 mM (Figure 4). The Job plot establishes a 1:1 ratio between **1** and 1,6-hexanediamine (**6**) within their complex (e.g., **1·6**). These results demonstrate that only a single molecule of **6** can complex with **1** at a time; putative ternary and higher-order complexes are unstable as a result of unfavorable electrostatic or steric interactions.

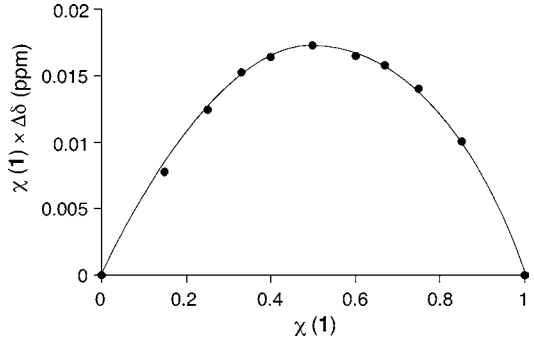

FIGURE 4. Job plot for CB[6] analogue (**1**) and 1,6-hexanediamine (**6**) on the basis of ^{1}H NMR experiments (400 MHz, 25 °C, 50 mM sodium acetate buffered D_2O, pD 4.74), monitoring the shift of the aromatic protons on the bis(phthalhydrazide) (H_a) of host **1**. The line in the graph is intended to act as a guide for the eye.

UV/Vis Study. As a result of the incorporation of the aromatic bis(phthalhydrazide) walls into the macrocycle, host **1** can also be monitored directly by spectroscopic techniques such as UV/vis and fluorescence. The ability to use optical detection methods is advantageous because the sensitivity of these techniques allows for the determination of large association constants of complexes in addition to the ability to monitor either the host or the guest, depending on the type of experiment. To assess the suitability of UV/vis as a general method to obtain **1**·guest binding constants, we performed a UV/vis titration experiment, monitoring the absorbance of the host at 330 nm (Figure 5) upon complexation with 1,6-hexanediamine (**6**) and compared the results to those based on the ^{1}H NMR measurements. As the concentration of **6** is increased in a solution containing a fixed concentration of **1**, a decrease in absorbance is observed. When we fit this change in absorbance to a 1:1 binding model by nonlinear least-squares analysis, we obtained an association constant of 370 ± 70 M^{-1}. The isosbestic point observed at ≈370 nm provides strong evidence for a clear two-state equilibrium in the system comprising **1** and **6**. Although the use of UV/vis spectroscopy to obtain association constants for **1** requires less material and less time than typical ^{1}H NMR titrations, the change in absorbance is small and for certain guests can prove impractical to monitor for accurate K_a determinations.

Fluorescence Studies. The use of fluorescence spectroscopy provides the easiest method to determine the association

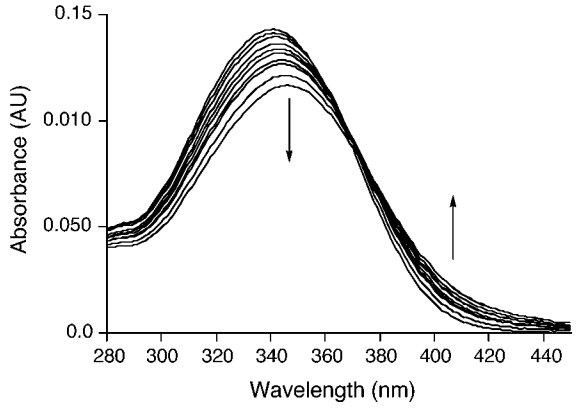

FIGURE 5. UV/vis titration of **1** (5.2 μM, 50 mM NaOAc, pH 4.74, 25 °C) with 1,6-hexanediamine (**6**; 0 mM − 10 mM).

constants of a variety of different guests with **1** because very small amounts of material are needed (2.5−25 μM), the data can be acquired rapidly, and the fluorescence spectrum shows a large change upon injection of a wide range of guests. Accordingly, as the concentration of **6** is increased in a solution containing a constant concentration of **1**, an increase in the fluorescence emission at 525 nm is observed (Figure 6a).[26] The change in the area under each fluorescence emission spectrum was determined by integration and then fit to a 1:1 binding model to give an association constant of 240 ± 12 M^{-1} (Figure 6b).[27] To further understand the factors which govern the binding of alkanediamines toward host **1**, we decided to examine the influence of chain length (n, $H_2N(CH_2)_nNH_2$) and functional group (e.g., OH vs NH_2) on the strength of binding with **1**.

Determination of Association Constants Using Fluorescence Spectroscopy. We chose to use fluorescence spectroscopy rather than ^{1}H NMR or UV/vis spectroscopy to determine the association constants of **1**·guest complexes for several reasons: (1) the data can be acquired quickly and accurately by directly monitoring the change in emission of **1**, (2) the amount of material needed is minimal as a result of the high sensitivity of fluorescence spectroscopy, (3) the change in the fluorescence emission spectrum of **1** is usually large and can be easily monitored for a wide range of guests, and (4) association constants on the order of 10^6 M^{-1} can be obtained directly.

Alkanediamines. To determine the influence of the length of the alkanediamines on the association constants, we performed fluorescence titrations with shorter and longer alkanediamines (**4**, **5**, **7**−**12**) and compared the results to those obtained for alkanediamine **6** (Chart 1). The general trend of decreasing binding affinity for different lengths of alkanediamines is as follows: 1,10-decanediamine (**10**) > 1,11-undecanediamine (**11**) > 1,12-dodecanediamine (**12**) > 1,9-nonanediamine (**9**) ≫ 1,8-octanediamine (**8**) > 1,7-heptanediamine (**7**) ≫ 1,6-hexanediamine (**6**).

Alkanediamine Lengths Influence Their Binding toward Host 1. As can be seen in Table 1, as the length of the alkyl chain increases, so does the binding constant. Once the length

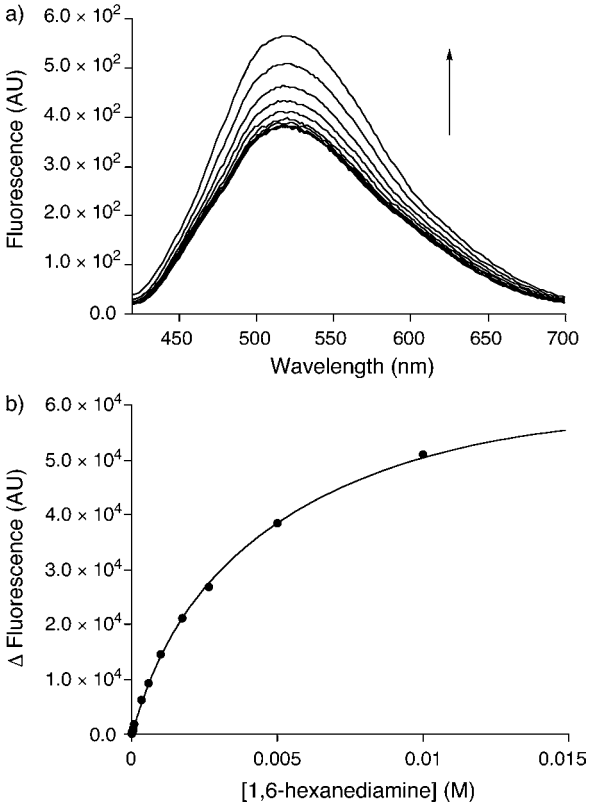

FIGURE 6. (a) Fluorescence titration of **1** (25 μM, 50 mM NaOAc, pH 4.74, 25 °C) with 1,6-hexanediamine (**6**; 0 mM − 10 mM). (b) A plot of the change in the integrated fluorescence emission (450−600 nm) of **1** versus [1,6-hexanediamine]; the solid line represents the best fit of the data to a 1:1 binding model with $K_a = (2.4 \pm 0.12) \times 10^2$ M^{-1}.

CHART 1. Alkanediamines and Alkanediols Used as Guests for 1. The Hydrogens Labeled on 1,6-Hexanediamine (6) Correspond with Their ^{1}H NMR Resonances in Figure 3

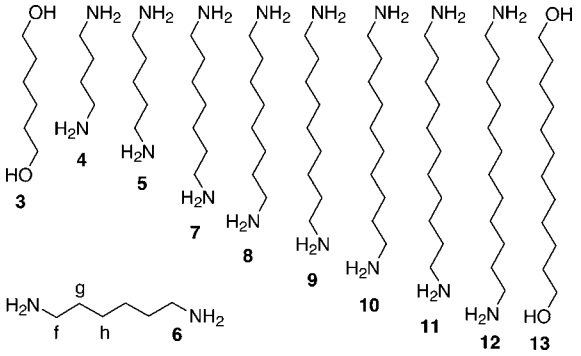

of the chain between the amines reaches 10 carbons, a maximum binding constant is reached at 24 000 M^{-1}. We hypothesize that unlike CB[6], which prefers to bind the shorter alkanediamines (**5** and **6**) that position their $-NH_3^+$ groups at the carbonyl-lined portals, CB[6] analogue **1** prefers the longer alkanediamines (**7**−**12**) as a result of the oval shape of the host, which maximizes both hydrophobic and ion−dipole interactions. On the basis of the binding constants of **6**−**12** with CB[6] analogue **1**, we hypothesize that the alkyl chain spans the hydrophobic cavity of the CB[6] analogue, as in the case of CB[6], but does so diagonally.

Figure 7 shows the results of a molecular mechanics force field (MMFF) minimization of the **1**·**10** complex. The hydro-

(26) Although we observe an increase in fluorescence upon the formation of the **1**·**6** complex, some host−guest complexes show a decrease in fluorescence. We do not fully understand the origin of these differences as a function of guest; this effect is the subject of ongoing study.

(27) The value of K_a determined for **1**·**6** by NMR, UV/vis, and flourescence titrations differs significantly. We attribute this discrepancy to the different media used (e.g., D_2O for NMR and H_2O for UV/vis and fluorescence) for the titrations.

TABLE 1. Association Constants for Guests 3−13 with 1, and Some Literature Values for CB[6]

guest	**1** K_a (M^{-1})	CB[6] K_a (M^{-1})[2]
3	n.d.[a]	n.r.[b]
4	n.d.[a]	1.5×10^5
5	n.d.[a]	2.4×10^6
6	$(2.4 \pm 0.12) \times 10^2$	2.8×10^6
7	$(2.8 \pm 0.12) \times 10^3$	4.3×10^4
8	$(5.4 \pm 0.17) \times 10^3$	9.0×10^3
9	$(1.8 \pm 0.05) \times 10^4$	4.8×10^2
10	$(2.4 \pm 0.33) \times 10^4$	1.0×10^2
11	$(2.3 \pm 0.27) \times 10^4$	n.r.[b]
12	$(2.0 \pm 0.27) \times 10^4$	n.r.[b]
13	n.d.[a]	n.r.[b]

[a] n.d. = no binding detected. [b] n.r. = not reported.

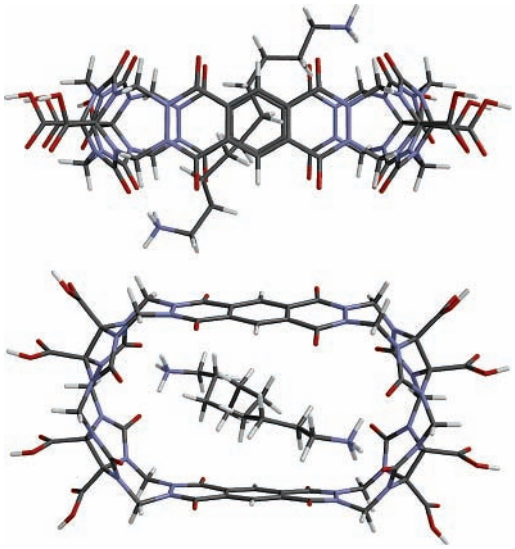

FIGURE 7. Minimized geometries for **1**·1,10-decanediammonium ion (**10**) obtained from MMFF calculations. Atom colors: C, gray; N, blue; O, red; and H, white.

phobic alkyl groups reside inside the cavity of the CB[6] analogue, shielded from the polar aqueous environment outside the cavity. As illustrated in Figure 7, the 1,10-decanediammonium ion is able to span across and through the cavity from one side of the macrocycle to the other to maximize the ion−dipole interactions between the ammonium groups and the carbonyls of the glycolurils as well as to fill the hydrophobic cavity more completely. Fluorescence titrations carried out using the shortest diamines, 1,4-butanediamine (**4**) and 1,5-pentanediamine (**5**), with CB[6] analogue **1** do not result in changes in the fluorescence spectrum. Thus, we conclude that the binding constant is significantly lower than that of 1,6-hexanediamine (**6**; $K_a < 240$ M^{-1}) and outside the dynamic range of the fluorescence measurements.[28]

Electrostatic Potential. Figure 8a shows the electrostatic potential energy map for CB[6];[8] the convergent C═O groups result in a highly electrostatically negative region at the two C═O lined portals. For comparison, Figure 8b shows the electrostatic potential calculated for CB[6] analogue **1**, which

(28) The lack of a change in the fluorescence spectrum does not rule out complex formation because the fluorescence spectrum of the host and the host·guest complex could accidentally be identical. To provide further evidence that 1,4-butanediamine (**4**) does not form a stable complex with host **1** under our experimental conditions, a ^{1}H NMR experiment was performed. Upon mixing **4** and **1**, there were no shifts in the resonances for either **4** or **1** in the NMR spectrum.

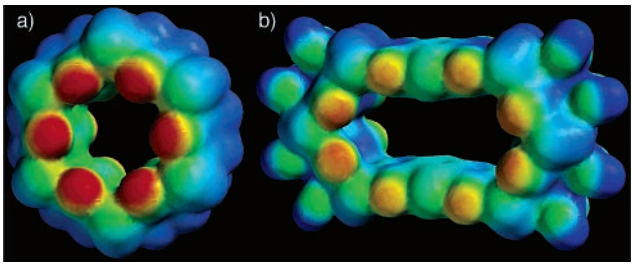

FIGURE 8. Electrostatic potential energy maps of (a) CB[6] and (b) CB[6] analogue **1**. The red to blue color range spans −78 to +35 kcal mol^{-1}.

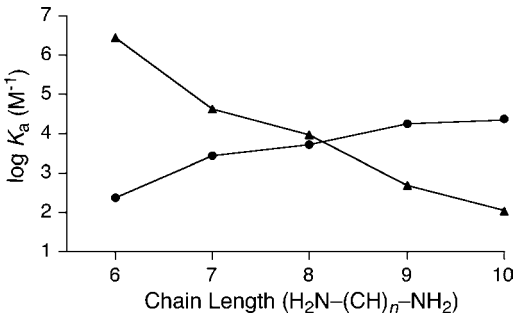

FIGURE 9. Relationship between the binding constant (log K_a) and the chain length *n* for alkanediamines **6**−**10** for CB[6] analogue **1** (●) and CB[6] (▲).[2]

indicates a less electrostatically negative portal comprising only four glycoluril carbonyl groups on each face of the macrocycle. These glycoluril carbonyl groups are important in the formation of favorable electrostatic interactions with the $-NH_3^+$ groups on the alkanediamine guest. The remaining four carbonyl groups associated with the bis(phthalhydrazide) portions of host **1** are significantly less electrostatically negative regions and are preferentially oriented parallel to the cavity of **1**. It is well-established that this electrostatic preorganization endows CB[6] with high selectivity toward the binding of alkanediamines. The less electrostatically negative portals of CB[6] analogue **1** are presumably a result of the fact that the four C═O groups on each side of **1** do not converge upon one another as dramatically as seen for CB[6]. Accordingly, we hypothesized that ion−dipole interactions would be less important in the recognition properties of **1** relative to CB[6] itself. The ability of the electron deficient bis(phthalhydrazide) side walls of **1** to engage in $\pi-\pi$ interactions will clearly play a prominent role in determining the affinity of **1** toward its guests.

CB[6] Shows Greater Selectivity toward the Binding of Alkanediamines Compared to that of Host 1. A comparison of the binding constants of alkanediamines (**6**−**10**) to CB[6] analogue **1** and CB[6] are illustrated in Figure 9. From this plot, it is immediately apparent that CB[6] possesses a higher affinity for alkanediamine **6** with an association constant on the order of 10^6 M^{-1}. On the other hand, CB[6] analogue **1** possesses a larger affinity for alkanediamines **9** and **10**, but with association constants on the order of 10^4 M^{-1}. Overall, CB[6] is a much better host for the binding of alkanediamines with association constants two orders of magnitude higher than that for CB[6] analogue **1**. This result is not surprising as a result of the fact that the shape of the cavities and portals are different. CB[6] possesses a barrel-like shape with all six electron-rich carbonyls pointed into the opening of the cavity slightly making it preorganized to engage in more favorable ion−dipole interac-

tions with alkanediamines. In addition to its higher affinity for alkanediamines, CB[6] is also a more selective receptor than **1** for these compounds. The selectivity of CB[6] for alkanediamines relative to CB[6] analogue **1** is evident by comparing the slope of the lines shown in Figure 9. For CB[6], the slope is much steeper (≈1.0 log K_a units per CH_2) than for CB[6] analogue **1** (≈0.6 log K_a units per CH_2) over a range of alkanediamines (**6**−**10**), which indicates that CB[6] displays better selectivity for shorter alkanediamines (e.g., **6**) versus longer alkanediamines (e.g., **10**) relative to host **1**.

After determining that **1** is capable of encapsulating alkanediamines in its cavity, we were curious to find out whether the amine groups on the alkanediamines were essential for binding to occur. Previous binding experiments with guests containing terminal hydroxy groups in place of ammonium groups have been shown to lead to a decrease in the affinity toward CB[6] of approximately 1000-fold.[3] This decrease in affinity is due to the absence of ion−dipole interactions in the case of −OH groups relative to $-NH_3^+$ groups.[2,10,29] Accordingly, we hypothesized that the affinity of **1** toward 1,6-hexanediol (**3**) would be significantly less favorable than **6** as a result of the lack of ion−dipole interactions in the complex. When the fluorescence titration experiment was carried out with host **1**, we did not observe a change in the fluorescence spectrum of **1** and thus conclude that the association constant between **1** and **3** is small, similar to what was observed for alkanediamines **4** and **5**. Finally, to further test whether the length of the alkanediamine and its resulting hydrophobicity is important in the formation of a stable host−guest complex with **1**, we used 1,12-dodecanediol (**13**). Once again, we did not observe a change in the fluorescence spectrum of **1** upon addition of **13**. Therefore, we can conclude that the ammonium groups, which interact with the carbonyl portals of host **1** through ion−dipole interactions, are essential for aliphatic guests to undergo tight binding in the cavity of **1**. The hydrophobic effect alone does not appear sufficient to induce tight binding with **1**. Protonated amino groups, which allow for ion−dipole interactions to occur spanning diagonally across the cavity of **1**, are the critical factor dictating the complexation of **1** with alkanediamines.

Affinity of Substituted Aromatic Guests toward CB[6] Analogue 1. The experimental results presented above led us to postulate that guests containing aliphatic chains are not the most favorable guests for **1** as a result of the fact that the advantageous $\pi-\pi$ interactions between host and guest cannot occur. Therefore, we sought to determine whether CB[6] analogue **1** is better suited to bind larger, specifically aromatic, guests. When CB[6] analogue **1** is compared to CB[6], which does not preferentially bind large aromatic molecules in its cavity, CB[6] analogue **1** possesses a wider cavity as well as the potential for $\pi-\pi$ interactions with the appropriate guests on the basis of the incorporation of aromatic walls into the macrocycle.

Previously, we determined that the binding constant of **1**·benzene (**14**) is 6900 M^{-1}.[21] The distance between the two aromatic walls in **1** is 6.9 Å, which results in a high level of preorganization for **1** to engage in favorable $\pi-\pi$ interactions with aromatic guests (Figure 2). On the basis of this relatively weak binding constant relative to the long-chain alkanediamines (**8**−**11**), we hypothesized that substituents with the ability to interact with **1** through ion−dipole interactions and hydrogen bonds, such as $-NH_3^+$ and −OH groups, would increase the affinity for these types of guests toward **1**. Also, increasing the size of the guests and the number of aromatic rings in the guest molecule should also increase the stability of these complexes. To determine whether CB[6] analogue **1** would display enhanced affinity toward a wider range of aromatic guests, fluorescence titration experiments were performed for several water-soluble aromatic compounds (Chart 2).

CHART 2. Aromatic Guests and Dyes Used in Fluorescence Titration Experiments with 1

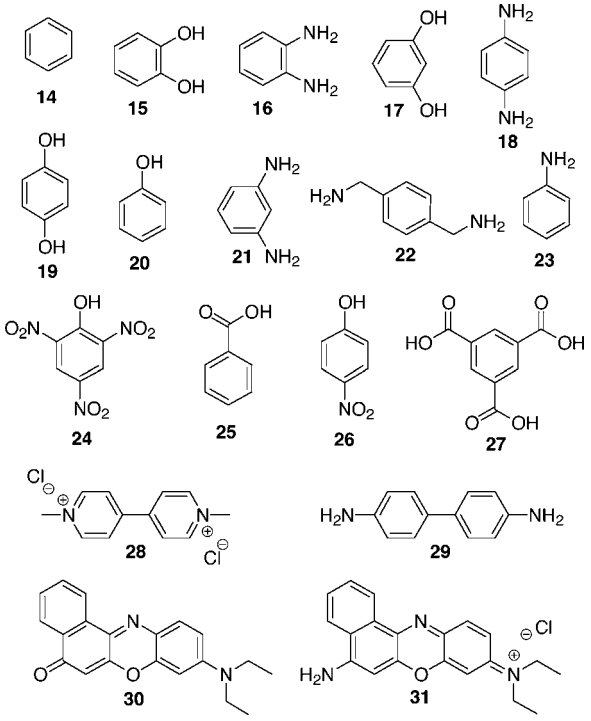

Accordingly, several guests were studied to give insight into the influence of electronics, sterics, number of hydrogen bond donors, and length/size of the different types of aromatic guests on complexation. From monosubstituted, to disubstituted, to trisubstituted aromatic compounds, the goal was to establish a structure−activity relationship between association constants and types of substituted aromatic molecules. The association constants range from 10^3 to 10^6 M^{-1} depending on the guest studied and were all obtained directly by monitoring the change in the emission of **1** through the use of fluorescence spectroscopy (Table 2). The order of decreasing binding affinity is as follows: catechol (**15**) > *o*-phenylenediamine (**16**) > resorcinol (**17**) > *p*-phenylenediamine (**18**) > hydroquinone (**19**) > phenol (**20**) > *m*-phenylenediamine (**21**) > *p*-xylylenediamine (**22**) > aniline (**23**) > picric acid (**24**) > benzoic acid (**25**) ≫ benzene (**14**) > *p*-nitrophenol (**26**).

Aromatic Guests Containing One Group Capable of Donating a H−Bond(s): Aniline, Phenol, Benzoic Acid. The association constant for aniline (**23**) is about one order of magnitude higher than benzene (**14**) at 4.5×10^4 M^{-1}. We hypothesize that this increased K_a is most likely a result of the anilinium $-NH_3^+$ group engaging in H-bonding and ion−dipole interactions with the carbonyls of **1**, similar to the alkanediamines discussed previously. Phenol (**20**) also has a larger affinity toward host **1** than benzene, which is most likely a result of the −OH group on the aromatic ring engaging in H bonding with the carbonyls of **1**.[30] These results provide evidence that

(29) Mock, W. L.; Shih, N. Y. *J. Am. Chem. Soc.* **1988**, *110*, 4706−4710.

TABLE 2. Association Constants of Aromatic Guests 14−31 with CB[6] Analogue 1, and Some Literature Values for CB[6] and CB[7]

guest	**1** K_a (M^{-1})	CB[*n*] K_a (M^{-1})[32]
14[21]	$(6.9 \pm 1.1) \times 10^3$	27 ($n = 6$)[33]
15	$(2.9 \pm 0.60) \times 10^5$	n.r.[b]
16	$(2.5 \pm 0.70) \times 10^5$	$(8.04 \pm 1.3) \times 10^4$ ($n = 7$)
17	$(1.3 \pm 0.20) \times 10^5$	n.r.[b]
18	$(8.0 \pm 1.4) \times 10^4$	1860 ± 100 ($n = 6$); $(2.07 \pm 0.33) \times 10^6$ ($n = 7$)
19	$(7.6 \pm 2.0) \times 10^4$	n.r.[b]
20	$(7.4 \pm 1.5) \times 10^4$	n.r.[b]
21	$(5.6 \pm 0.80) \times 10^4$	$(8.07 \pm 0.60) \times 10^4$ ($n = 7$)
22	$(5.4 \pm 0.30) \times 10^4$	550 ± 30 ($n = 6$); $(1.84 \pm 0.34) \times 10^9$ ($n = 7$)
23	$(4.5 \pm 0.70) \times 10^4$	5.3×10^3 ($n = 6$)
24	$(3.8 \pm 0.40) \times 10^4$	n.r.[b]
25	$(2.5 \pm 0.50) \times 10^4$	n.r.[b]
26	$(2.5 \pm 0.30) \times 10^3$	n.r.[b]
27	n.d.[a]	n.r.[b]
28	$(2.2 \pm 0.08) \times 10^4$	$(1.32 \pm 0.21) \times 10^7$ ($n = 7$)
29	$(4.6 \pm 1.8) \times 10^6$	n.r.[b]
30[21]	$(8.2 \pm 0.50) \times 10^6$	n.r.[b]
31	$(1.1 \pm 0.20) \times 10^6$	n.r.[b]

[a] n.d. = no binding detected. [b] n.r. = not reported.

the addition of groups to the aromatic ring of the guest molecule, which can form hydrogen bonds or ion−dipole interactions with the electron-rich carbonyl portals of **1**, have a greater affinity for **1** with binding constants in the range of 10^4 M^{-1}, which is approximately one order of magnitude higher than the unsubstituted benzene (**14**). The combination of these noncovalent interactions, which are not available with benzene (**14**), leads to an increase in the association constant for aniline (**23**) and phenol (**20**). On the other hand, benzoic acid (**25**) has a smaller association constant ($K_a = 2.5 \times 10^4$ M^{-1}) relative to aniline (**23**) but a larger association constant relative to benzene (**14**). On the basis of the decrease of the association constant of benzoic acid (**25**) relative to aniline (**23**) and phenol (**20**), we hypothesize that the $-CO_2H$ group is better solvated, making the guest less hydrophobic, which leads to less favorable host−guest interactions.[31]

Aromatic Guests Containing Two Groups Capable of Donating H−Bonds. Additional substitution on the aromatic ring of the guests generally increases the association constant toward CB[6] analogue **1**. Specifically, catechol (**15**) and *o*-phenylenediamine (**16**) have very favorable interactions with **1** on the basis of their association constants of 2.9×10^5 and 2.5×10^5 M^{-1}, respectively (Table 2). These results provide evidence that ortho-substituted aromatic rings bind preferentially in the cavity of **1** relative to *para*-substituted aromatic rings. On the basis of the minimized geometries for catechol (**15**) obtained from MMFF calculations (Supporting Information), one of the −OH groups hydrogen bonds with the carbonyls of the glycolurils, while the other −OH forms an intramolecular hydrogen bond. A similar geometry and enhanced K_a is observed for *o*-phenylenediamine (**16**) relative to *p*-phenylenediamine (**18**). Meta-substituted resorcinol (**17**) forms a strong complex with **1** ($K_a = 1.3 \times 10^5$ M^{-1}), but the K_a value for the corresponding *meta*-diamine **21** is reduced by half (K_a (**1**·**21**) $= 5.6 \times 10^4$ M^{-1}). Currently, we do not understand the origin of this difference between **17** and **21**. We would expect a higher binding constant on the basis of the ability of **21** to participate in H bonding and $\pi-\pi$ interactions as well as the additional ion−dipole interactions due to the $-NH_3^+$ groups. On the other hand, the electron-rich aromatic ring of **17** can form favorable charge-transfer interactions with the electron-poor bis(phthalhydrazide) walls while inside the cavity of **1**.[34] Apparently, a fine balance exists between the various factors, $\pi-\pi$, ion−dipole, charge-transfer, and H-bonding interactions, which determine the stability of **1**·guest complexes.

Aromatic Guests Containing Multiple Functional Groups: 1,3,5-Benzenetricarboxylic Acid, *p*-Nitrophenol, and Picric Acid. We chose to study the ability of trisubstituted 1,3,5-benzenetricarboxylic acid (**27**) to bind inside the cavity of host **1**. Fluorescence titration of **1** with **27** did not show a change in the fluorescence emission spectrum of **1**. We postulate that the increase in the number of the $-CO_2H$ groups increases the solvation of the guest, which makes the guest less hydrophobic, thus, a decrease in the K_a with **1** is observed.[32,35] Therefore, the addition of two $-CO_2H$ groups on the aromatic ring dramatically decreases the association constant between **1** and **27** relative to benzoic acid (**25**). We postulate that benzoic acid (**25**) can form favorable $\pi-\pi$ interactions in the cavity of **1** simply by directing the $-CO_2H$ group away from the cavity, whereas trisubstituted **27** does not have the ability of placing all three $-CO_2H$ groups away from the carbonyls on host **1** and outside the hydrophobic cavity of **1**.

The detection of explosives in soil and groundwater has been explored using host−guest chemistry on the basis of self-assembled monolayers functionalized with cyclodextrins.[36] The ability of **1** to bind nitrated arenes was, therefore, investigated to determine whether the CB[6] analogue **1** might be used in detecting explosives such as trinitrotoluene (TNT) and dinitrotoluene (DNT). We used *p*-nitrophenol (**26**) and picric acid (**24**) as surrogates for determining the relative affinity of nitrated arenes toward **1** because they are not highly explosive and they possess better solubilities in aqueous solutions than TNT and DNT. When fluorescence spectroscopy was used, we were able to determine the association constants of *p*-nitrophenol (**26**) and picric acid (**24**) with CB[6] analogue **1**. The association constants for **26** and **24** are 2.5×10^3 and 3.8×10^4 M^{-1}, respectively. We hypothesize that the enhancement in the binding relative to **26** is due to the favorable $\pi-\pi$ interactions between the electron-poor walls of the host and the electron-poor arene. The size and shape of the 1,3,5-trinitro-substituted aromatic ring is a good match for the cavity of **1**; this result bodes well for the use of **1** as a fluorescent sensor for explosive devices based on TNT.

(30) Alternatively, the electron-rich aromatic ring of **20** may engage in enhanced $\pi-\pi$ interactions or charge-transfer type interactions with host **1**.

(31) Alternatively, the less electron-rich aromatic ring may engage in more favorable $\pi-\pi$ interactions with **1** relative to **14**.

(32) Liu, S.; Ruspic, C.; Mukhopadhyay, P.; Chakrabarti, S.; Zavalij, P. Y.; Isaacs, L. *J. Am. Chem. Soc.* **2005**, *127*, 15959−15967.

(33) Jeon, Y.-M.; Kim, J.; Whang, D.; Kim, K. *J. Am. Chem. Soc.* **1996**, *118*, 9790−9791.

(34) Kim, H.-J.; Heo, J.; Jeon, W. S.; Lee, E.; Kim, J.; Sakamoto, S.; Yamaguchi, K.; Kim, K. *Angew. Chem., Int. Ed.* **2001**, *40*, 1526−1529. Jeon, Y. J.; Bharadwaj, P. K.; Choi, S. W.; Lee, J. W.; Kim, K. *Angew. Chem., Int. Ed.* **2002**, *41*, 4474−4476.

(35) Alternatively, **27** will be partially anionic at pH 4.74; electrostatic interactions are known to strongly influence the affinity of CB[*n*]·guest interactions. Jeon, W. S.; Moon, K.; Park, S. H.; Chun, H.; Ko, Y. H.; Lee, J. Y.; Lee, E. S.; Samal, S.; Selvapalam, N.; Rekharsky, M. V.; Sindelar, V.; Sobransingh, D.; Inouye, Y.; Kaifer, A. E.; Kim, K. *J. Am. Chem. Soc.* **2005**, *127*, 12984−12989.

(36) Swanson, B. I.; Shi, J.; Johnson, S.; Yang, X. *Proc. SPIE−Int. Soc. Opt. Eng.* **1998**, *3270*, 25−31. Yang, X.; Du, X. X.; Shi, J.; Swanson, B. *Talanta* **2001**, *54*, 439−445. Sheremata, T. W.; Hawari, J. *Environ. Sci. Technol.* **2000**, *34*, 3462−3468.

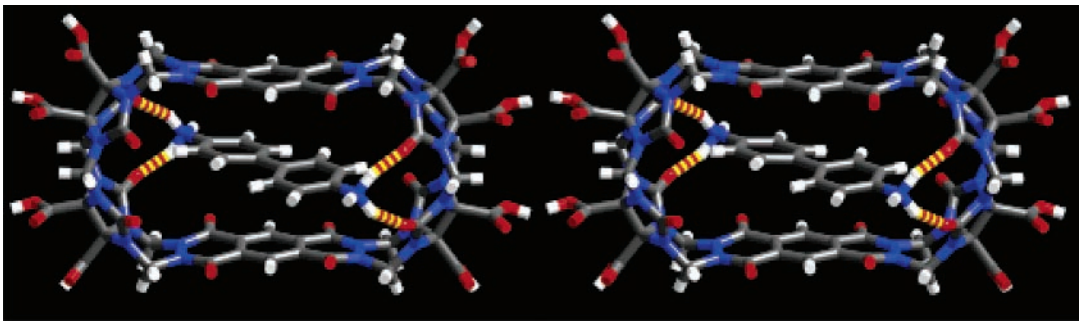

FIGURE 10. Cross-eyed stereoview of the MMFF-minimized structure of **1**·benzidine (**29**). Atom colors: C, gray; N, blue; O, red; and H, white; H bonds are red-yellow striped.

Larger Aromatic Guests Increase the Surface Area of $\pi-\pi$ Interactions. On the basis of the binding constant of CB[6] analogue·guest complexes being strongly dependent on the nature (e.g., number and pattern of functional groups) of the aromatic guest, we decided to study guests that possess two or more aromatics rings in their structure. Methyl viologen (**29**) has been used previously to study the molecular-recognition properties of both CB[7] and CB[8].[32,37] CB[7] forms a 1:1 complex with **28** ($K_a = 1.3 \times 10^7$ M^{-1}), which is approximately three orders of magnitude larger than the formation of **1**·**28** ($K_a = 2.2 \times 10^4$ M^{-1}). We postulate that this difference in K_a is due to CB[7] possessing an appropriately sized and shaped cavity for **28**, which maximizes the noncovalent interactions compared to that of CB[6] analogue **1**. CB[8] forms a 1:1 complex with **28** ($K_a = 1.1 \times 10^5$ M^{-1}) that is less stable than CB[7]·**28**, indicating that the distance spanning from one C=O portal to the other provides favorable ion−dipole interactions with the pyridinium rings in the formation of both 1:1 complexes (CB[7]·**28** and CB[8]·**28**), but the size of the cavity of CB[7] accommodates guest **28** better, resulting in the formation of a tighter complex.

Accordingly, we hypothesized that benzidine (**29**) would be an ideal guest for **1** on the basis of molecular mechanics calculations. The distance between the $-NH_2$ groups of **29** is similar to 1,10-decanediamine (**10**), and the aromatic rings provide a rigidity to the guest as well as the possibility to interact with the aromatic walls of the host through $\pi-\pi$ interactions. As can be seen in Figure 10, **29** is capable of spanning the hydrophobic cavity of **1** with favorable $\pi-\pi$ interactions as well as ion−dipole interactions of the protonated amines with the carbonyls on the glycolurils of the macrocycle. As expected, there is a slight twist between the biphenyl rings in **29** as it is bound in the cavity of host **1**. This twist in guest **29** while bound in the cavity of **1** results in a slight twist in the bis(phthalhydrazide) walls of host **1** to maximize the $\pi-\pi$ interactions with **29**. From this minimized structure, the distance from the center of the Ar−Ar bond of the guest to the centroid of the aromatic ring of the host is ≈3.4 Å, which is consistent with the preferred distance for $\pi-\pi$ interactions. After performing the fluorescence titration experiment, we discovered that the association constant for **1**·**29** was 4.6×10^6 M^{-1}. This result was comparable to that obtained for nile red (**30**), which binds with an association constant of 8.2×10^6 M^{-1}.[21] On the basis of the strong affinity of the dye **30**, we decided to study a similar dye called nile blue chloride (**31**), which resulted in a similar association constant of 1.1×10^6 M^{-1}. These results provide evidence, as expected, that increasing the surface area for $\pi-\pi$ interactions by increasing the size of the π system of the guest as well as increasing the coplanarity of the guest molecule significantly increases the association constant. Accordingly, host **1** functions as an excellent receptor for dyes and other large, flat aromatic molecules. These results suggest that CB[6] analogue **1** will become a broadly applicable host for the detection of polycyclic aromatics with detection limits approaching or exceeding the μM range. Through the judicious selection of guests with complementary size and shape as well as electrostatic profile, it is possible to obtain host−guest complexes of **1** with K_a values that exceed 10^6 M^{-1}!

CHART 3. Biologically Relevant Guests Used To Investigate the Binding Properties of CB[6] Analogue 1

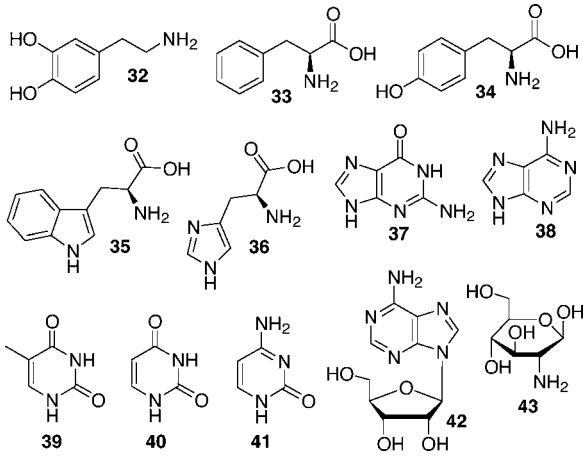

Biologically Relevant Guests Bind in the Cavity of Host 1. As a result of the high solubility of host **1** in aqueous solutions, its high affinity toward aromatic molecules, and the ability to detect these guest molecules at μM concentrations with fluorescence spectroscopy, we envisioned **1** as a potential module for use in applications such as ion and molecular transport as well as peptide and DNA sensing. Importantly, proteins and DNA do not absorb at long UV/vis wavelengths and, therefore, do not interfere with the detection of host **1**. To test our hypothesis that CB[6] analogue **1** would associate with biological molecules, we chose to study several amino acids and nucleobases (Chart 3). These experiments were performed using fluorescence spectroscopy to monitor the change in the fluorescence emission of host **1**, as described above.

(37) Jeon, W. S.; Kim, H.-J.; Lee, C.; Kim, K. *Chem. Commun.* **2002**, 1828−1829. Ong, W.; Gomez-Kaifer, M.; Kaifer, A. E. *Org. Lett.* **2002**, *4*, 1791−1794. Ong, W.; Kaifer, A. E. *Angew. Chem., Int. Ed.* **2003**, *42*, 2164−2167. Ong, W.; Kaifer, A. E. *J. Org. Chem.* **2004**, *69*, 1383−1385. Moon, K.; Kaifer, A. E. *Org. Lett.* **2004**, *6*, 185−188.

TABLE 3. Association Constants of Biologically Relevant Guests 32−43 with CB[6] Analogue 1

guest	**1** K_a (M^{-1})	CB[7] K_a (M^{-1})[32]
32	$(7.1 \pm 0.60) \times 10^4$	$(4.32 \pm 0.68) \times 10^4$
33	$(4.2 \pm 0.70) \times 10^4$	$(1.45 \pm 0.23) \times 10^5$
34	$(5.7 \pm 1.1) \times 10^4$	n.r.[c]
35	$(3.2 \pm 1.0) \times 10^6$	n.r.[c]
36	n.d.[a]	n.r.[c]
37	n.s.[b]	n.r.[c]
38	$(4.4 \pm 0.90) \times 10^4$	n.r.[c]
39	$(3.8 \pm 0.90) \times 10^3$	n.r.[c]
40	$(6.0 \pm 1.0) \times 10^3$	n.r.[c]
41	$(7.0 \pm 1.4) \times 10^3$	n.r.[c]
42	n.d.[a]	n.r.[c]
43	n.d.[a]	n.r.[c]

[a] n.d. = no binding detected. [b] n.s. = not soluble. [c] n.r. = not reported.

Dopamine. On the basis of the high affinity of **1** toward catechol (**15**), we decided to study the binding of dopamine (Chart 3, **32**), which is similar to **15** but possesses a $-(CH_2)_2$-NH_2 group on the aromatic ring. Under our experimental conditions (pH 4.74), the amino group is protonated, which should enhance the K_a value for **1·32** by the combined influence of ion−dipole, hydrogen-bonding, and $\pi-\pi$ stacking interactions. In the experiment, we found that the K_a value ($K_a = 7.1 \times 10^4$ M^{-1}) is comparable to that observed for **1·15**. We postulate that the geometrical preferences of the catechol (**15**) and ammonium regions of guest **32** are incompatible and result in an overall decrease in the association constant. Specifically, the $-NH_3^+$ of dopamine (**32**) would like to position itself at either one of the carbonyl portals of host **1**, similar to the alkanediamines discussed previously, to maximize the ion−dipole interactions and hydrogen bonding. For this conformation of binding to occur, the complex must sacrifice more favorable $\pi-\pi$ interactions as well as hydrogen bonding with one of the −OH groups on the aromatic portion of **32** (see Supporting Information). On the other hand, if the aromatic portion of **32** is positioned in the cavity to maximize the $\pi-\pi$ interactions within the cavity of **1**, the $-NH_3^+$ group is unable to form favorable interactions with the carbonyl portal of host **1**. The ability of **1** to detect **32** in water has several potentially significant biological uses because dopamine is an important neurotransmitter.

Aromatic Amino Acids Form Strong Complexes with CB[6] Analogue 1. Fluorescence titration experiments were also performed with L-phenylalanine (**33**), L-tyrosine (**34**), and L-tryptophan (**35**). We chose these aromatic amino acids because host **1** should possess good affinity for them as a result of $\pi-\pi$ stacking and ion−dipole interactions. Compounds **33**−**35** have association constants of 4.2×10^4, 5.7×10^4, and 3.2×10^6 M^{-1}, respectively (Table 3). CB[6] analogue **1** binds **35** especially tightly, which is most likely a result of the larger size of the indole ring compared to that of the monocyclic rings on amino acids **34** and **35**. On the basis of these initial results, we believe that CB[6] analogue **1** will bind to peptides and proteins containing aromatic amino acid residues, which will be useful in peptide-sensing applications. Interestingly, when the titration was performed using L-histidine (**36**) as a guest, the fluorescence emission spectrum of **1** did not change. In the case of **36**, we hypothesize that the protonation of the imidazole ring N atom makes the aromatic ring relatively hydrophilic. Apparently, the removal of the solvating water molecules is less favorable than guest inclusion within the cavity of **1**. A similar result was recently reported by Urbach for the complexation of **36** inside CB[8]·**28**. In this study, Urbach also reports of the binding of **33**−**35** toward CB[8]·**28**, with binding constants of 5.3×10^3, 2.2×10^3, and 4.3×10^4 M^{-1}, respectively, at 27 °C in sodium phosphate (10 mM, pH 7.0).[18] In combination, these experiments provide evidence that the hydrophobicity of the aromatic portion of the amino acid is essential to complexation inside the hydrophobic cavity of **1**.

Overall, CB[6] analogue **1** possesses a slightly larger affinity for guests **33**−**35** compared to CB[8]·**28** as a result of **1** possessing two aromatic walls in the macrocycle that can participate in a sandwich-like binding (dual $\pi-\pi$ interactions) where the aromatic walls are on both sides of the aromatic guest, whereas CB[8]·**28** can only interact with one side of the aromatic guest (single $\pi-\pi$ interaction). Although the affinities of **1** and CB[8]·**28** are comparable, it may be advantageous to use **1** in certain cases because **1**, with its native fluorescence, will be responsive at sub-μM concentration where CB[8]·**28** will dissociate into CB[8] and **28**, which do not exhibit a fluorescence response to amino acids.

Nucleobases as Guests for CB[6] Analogue 1. We were also interested in the potential binding of the building blocks of RNA and DNA, therefore, we studied the ability of CB[6] analogue **1** to bind all five of the different nucleobases (Chart 3).[38] Unfortunately, guanine (**37**) was not soluble in the media used for our binding experiments (sodium acetate, 50 mM, pH 4.74, 25 °C), so we were unable to determine its association constant with **1**. However, the other purine, adenine (**38**), and the pyrimidines, thymine (**39**), uracil (**40**), and cytosine (**41**), were all soluble, which facilitated the determination of their affinity toward CB[6] analogue **1** (Table 3). Not surprisingly, **38**, with its large π surface relative to the pyrimidines, has the largest association constant ($K_a = 4.4 \times 10^4$ M^{-1}) of the nucleobases studied. All the pyrimidines have relatively small association constants on the order of 10^3 M^{-1}. Interestingly, adenosine (**42**) does not bind to host **1**. We postulate that sterics and solvation effects are important factors in the binding process to form stable host−guest complexes with CB[6] analogue **1**. The sugar residue of **42** most likely makes the guest too bulky as well as more hydrophilic (relative to adenine (**38**)) to bind efficiently in the cavity of **1**. To provide further evidence that sugars do not associate with host **1**, glucosamine (**43**) was injected into a solution containing **1**; no binding was detected by fluorescence spectroscopy. From these experiments, we conclude that nucleosides as well as sugars do not possess the appropriate shape or hydrophobicity necessary to form stable complexes with host **1**.

Conclusion

In summary, we have described the incorporation of (bis)-phthalhydrazide walls into the macrocycle of CB[6] analogue **1**, which gives rise to its fluorescent properties. The size and shape of **1** permits the binding of larger, flatter guests relative to the parent CB[6] while still retaining the ability to bind long chain alkanediamines, although with distinct geometrical preferences. The combination of noncovalent interactions, such as $\pi-\pi$ stacking, ion−dipole, and hydrogen-bonding, and the hydrophobic effect results in efficient complexation of a wide variety of guests within CB[6] analogue **1**. For example,

(38) Kim, K.; Balaji, R.; Oh, D.-H.; Ko, Y.-H.; Jon, S.-Y. *PCT Int. Appl.* WO 2004072151, 2004 (Postech Foundation, S. Korea); *Chem. Abstr.* **2004**, *141*, 207238.

CB[6] analogue **1** forms tight complexes ($K_a \approx 10^6$ M^{-1}) with nitro aromatics, amino acids, dyes, neurotransmitters, and even nucleobases. Consequently, CB[6] analogue **1** functions as a versatile fluorescence sensor for a variety of chemically and biologically important species in water with detection limits in the μM range.

Although we focus in this paper on the interactions of **1** with aromatic amino acids (e.g., tryptophan (**35**)) and nucleobases (e.g., adenine (**38**)), CB[6] analogue **1** should retain the ability to bind to these residues even when incorporated into larger macromolecular structures such as peptides and proteins. In addition, the studies described herein were limited to octacarboxylic acid **1**; the carboxylic groups on the equator of **1** can be functionalized to yield organic soluble CB[*n*] analogues, which may display intriguing recognition properties in lipophilic environments.[39] These carboxylic groups may also function as handles for the attachment of **1** to solid supports (e.g., glass slides or polymer resins), which would allow the detection and separation of aromatic guests including, but not limited to, dyes, peptides, and explosives. With their straightforward detection by UV/vis and fluorescence spectroscopy, their ability to recognize several types of aromatic guests with affinities up to 10^6 M^{-1} CB[6] analogue **1** and its relatives family, and their ease of functionalization, these macrocycles may be applied in a variety of practical sensing applications.

Experimental Section

^{1}H NMR Spectroscopy. For ^{1}H NMR experiments, solutions were prepared in NaOAc buffered D_2O (pD = 4.74, 50 mM). All spectra were recorded on a spectrometer operating at 400 MHz for ^{1}H and are referenced to external $(CH_3)_3SiCD_2CD_2CO_2H$ ($\delta = 0.0$ ppm). The temperature was calibrated using the separation of the resonances of $HOCH_2CH_2OH$ and controlled at 22 ± 1 °C using a temperature control module. The chemical shifts of host **1** were monitored as a function of added 1,6-hexanediamine concentration, and the tabulated values of chemical shift versus concentration were used to determine values of K_a by nonlinear least-squares analysis using Associate 1.6.[40] For the Job plot, the total concentration of host **1** and 1,6-hexanediamine was held constant at 1 mM. As the mole fraction (χ) of host **1** was changed from 0 to 1.0, the chemical shifts of the resonances for the host were monitored. The Job plot was constructed using the mole fraction (χ) of host **1** × the change in chemical shift ($\Delta\delta$) versus the mole fraction (χ) of host **1**.

UV/Vis Spectroscopy. Solutions for UV/vis titrations were prepared in NaOAc buffer (pH 4.74, 50 mM). All spectra were measured on a UV−visible spectrophotometer using 1-cm path length quartz cuvettes. The temperature was maintained at 22 ± 1 °C using a microprocessor controlled recirculator bath. The change in absorbance of host **1** was monitored at 340 nm as a function of increasing 1,6-hexanediamine concentration, and the change in absorbance versus concentration was used to determine values of K_a by nonlinear least-squares analysis fitting to a 1:1 binding model.

Fluorescence Spectroscopy. Solutions for fluorescence titrations were prepared in NaOAc buffer (pH 4.74, 50 mM). All spectra were measured on a fluorescence spectrophotometer with excitation and emission monochromator band passes set at 5 nm. The temperature was held constant at 22 ± 1 °C using a RTE bath/circulator containing a microprocessor controller. An excitation wavelength of 360 nm was used for the fluorescence of host **1**. The change in fluorescence emission was monitored as a function of increasing guest concentration, and the area under each spectrum was determined by integration from 450 to 600 nm. The change in area under the emission spectra versus the guest concentration was used to determine the values of K_a by nonlinear least-squares analysis fitting to a 1:1 binding model.

Computational Results. Minimized geometries obtained from molecular mechanics calculations were performed using commercial software packages employing the MMFF. Electrostatic potentials were determined by single-point calculations (PM3) of the MMFF-minimized geometries of **1** and CB[6].

Acknowledgment. We thank the University of Maryland and the NIH (GM61854) for generous financial support.

Supporting Information Available: Fluorescence titration spectra and nonlinear least-squares analysis fitting to a 1:1 binding model for selected guests with host **1** as well as minimized geometries obtained from MMFF calculations for selected complexes. This material is available free of charge via the Internet at http://pubs.acs.org.

JO052294I

(39) Jeon, J. J.; Kim, H.; Jon, S.; Selvapalam, N.; Oh, D. H.; Seo, I.; Park, C.-S.; Jung, S. R.; Koh, D.-K.; Kim, K. *J. Am. Chem. Soc.* **2004**, *126*, 15944−15945.

(40) Peterson, B. R. Ph.D. Dissertation, University of California, Los Angeles, CA, 1994.